J Surg Med. 2023;7(9):584-589.
DOI: 10.28982/josam.7916

Research article

Journal of Surgery and Medicine
e-ISSN: 2602-2079
https://jsurgmed.com/

Volumetric apparent diffusion coefficient histogram analysis for determining the degree of differentiation of periampullary carcinomas

Mustafa Orhan Nalbant, Ercan Inci

University of Health Sciences, Bakirkoy Dr. Sadi Konuk Training and Research Hospital, Department of Radiology, Istanbul, Turkey

ORCID ID of the author(s)

MON: 0000-0002-5277-9111
EI: 0000-0002-3791-2471

Corresponding Author
Mustafa Orhan Nalbant
University of Health Sciences, Bakirkoy Dr. Sadi Konuk Training and Research Hospital, Department of Radiology, Tevfik Saglam Cad. No:11 Zuhuratbaba 34147, Bakırkoy, Istanbul, Turkey
E-mail: musnalbant88@hotmail.com

Ethics Committee Approval
The study was approved by the Ethics Committee at Bakirkoy Dr. Sadi Konuk Training and Research Hospital of the University of Health Sciences on April 11, 2023 (Decision No: 2023/94).
All procedures in this study involving human participants were performed in accordance with the 1964 Helsinki Declaration and its later amendments.

Conflict of Interest
No conflict of interest was declared by the authors.

Financial Disclosure
The authors declared that this study has received no financial support.

Published
2023 September 19

Abstract

Background/Aim: The classification of periampullary adenocarcinomas into pancreatobiliary-type periampullary adenocarcinoma and intestinal-type periampullary adenocarcinoma (PPAC and IPAC, respectively) has gained significant acceptance in the medical community. A patient's prognosis is determined by the degree of differentiation of these tumor types. The objective of the present investigation was to assess the efficacy of volumetric apparent diffusion coefficient (ADC) histogram analysis in assessing the degree of differentiation for these two tumor types.
Methods: This retrospective cohort research evaluated 54 PPAC (45 well-differentiated and nine poorly differentiated) and 15 IPAC (11 well-differentiated and four poorly differentiated) patients. Magnetic resonance imaging (1.5 T MRI) scans were used to evaluate the results. The features of the histogram for the ADC values were computed and incorporated several statistical measures, such as the mean, minimum, median, maximum, and percentiles in addition to the skewness, kurtosis, and variance.
Results: In both PPAC and IPAC patients, the ADC values exhibited lower values in the poorly differentiated group when compared with the well-differentiated group. However, the changes between groups did not reach statistical significance. Among IPAC patients, the well-differentiated group had a larger kurtosis (P=0.048). In IPAC patients, the calculated value for the area under the curve (AUC) of kurtosis was determined to be 0.818. When the threshold was set at 0.123, the specificity and sensitivity were observed to be 90% and 75%, respectively.
Conclusion: Our research indicates that the kurtosis of ADC is an effective indicator to determine the level of IPAC differentiation. Analysis of the histogram at increased b values can provide valuable insights to help determine the degree of differentiation of IPAC using a noninvasive technique.

Keywords: apparent diffusion coefficient, differentiation degree, periampullary adenocarcinoma, volumetric histogram

How to cite: Nalbant MO, Inci E. Volumetric apparent diffusion coefficient histogram analysis for determining the degree of differentiation of periampullary carcinomas. J Surg Med. 2023;7(9):584-589.

Introduction

Periampullary adenocarcinoma (PAC) includes pancreatic ductal adenocarcinoma (PDAC), distal cholangiocarcinoma, ampullary carcinoma, and duodenal adenocarcinoma and accounts for 5% of all gastrointestinal tract malignancies [1]. Pancreatic head adenocarcinoma is the most frequent source of periampullary-type malignancies. However, pre-operative imaging differentiation between these origins is difficult due to their close anatomical proximity. The primary tumor origin affects patient prognosis and survival rates. Consequently, pathological evaluation is frequently required [2].

In over 50% of cases, PDAC is typically detected in its advanced stages, and despite advancements in treatment approaches, the 5-year relative survival rate remains around 20%. Early detection of patients who are eligible for curative surgery is limited to around 15% of cases to be performed immediately [3]. Although a considerable proportion of patients who have undergone surgical resection for PDAC experience the development of both local and systemic metastases, which ultimately lead to mortality within the initial year post-surgery, improvements in adjuvant therapies have been associated with an increase in survival [4,5]. The ampullary area is characterized by its intricate nature. Misdiagnosis of the primary tumor site could indeed occur during clinical practice [6]. A new classification was introduced to divide adenocarcinomas into two subtypes based on their histological differentiation: (1) pancreatobiliary-type periampullary adenocarcinoma (PPAC) and (2) intestinal-type periampullary adenocarcinoma (IPAC). This classification is now widely accepted for identifying periampullary adenocarcinomas [7].

Pancreatoduodenectomy is utilized to treat periampullary adenocarcinomas that are resectable. However, this treatment varies based on the survival rates and the histological characteristics of the adenocarcinoma's genesis [8]. Assessing the prognosis of patients with resectable periampullary adenocarcinomas is one of the greatest concerns when attempting to bring about a decrease in the need for unwarranted surgical interventions in individuals with a high probability of early tumor recurrence. The precise etiology of early recurrence is not completely understood but presumably involves histological and genetic tumor heterogeneity with micrometastases that remain imperceptible by imaging techniques even in cases in which they are amenable to surgical removal. Regrettably, the genetic characteristics of PAC can only be evaluated based on histological specimens, which are often not obtained for resectable adenocarcinomas [9–11]. Hence, it would be advantageous if non-invasive techniques could enhance the prognostic classification of such individuals.

Histogram analysis is an efficient method for the analyzing the spread of levels of gray within a specific region of interest (ROI) on cross-sectional images that can be used by employing descriptive characteristics. Analysis of these histograms can provide useful information concerning gene expression, angiogenesis, metabolism, and tumor heterogeneity [12]. Variations in histogram parameters represent histological and functional distinctions in tumor composition that are associated with aggressiveness and prognosis; these may be applicable to treatment alternatives. Diffusion-weighted imaging (DWI) is a type of magnetic resonance imaging (MRI) that measures the phenomenon of Brownian motion, which refers to the random movement exhibited by water molecules within a tissue voxel. Whole-lesion volumetric histogram assessment eliminates ROI placement subjectivity to assure consistency and computation accuracy, a technique that may eliminate sampling bias [13].

To our knowledge, only one study that includes apparent diffusion coefficient (ADC) histogram analysis for PPAC and IPAC without involving the degree of differentiation of periampullary adenocarcinomas is available [14]. Our objective was to evaluate the usefulness of the analysis of volumetric ADC histograms for differentiating between degrees of differentiation in PPAC and IPAC.

Materials and methods

The retrospective cohort research was approved by the Human Subjects Ethics Committee at the Bakirkoy Dr. Sadi Konuk Training and Research Hospital of the University of Health Sciences on April 11, 2023 (Decision No: 2023/94). Moreover, the guidelines of the Helsinki Declarations were followed. One-hundred eighty-two patients were evaluated for the study between July 2015 and January 2023. Among them, 113 patients were excluded. The exclusion criteria for these patients are summarized in Table 1. The study comprised 69 patients who were histopathologically diagnosed with PPAC (54 patients) or IPAC (11 patients) following surgery and who underwent pre-operative MRI. The time interval between the pre-operative MRI and the surgical procedure varied from 7 to 15 days. Patients were classified into two subgroups (well-differentiated and poorly differentiated) based on their degree of differentiation. Patients with moderately differentiated histopathology were included in the well-differentiated group.

Table 1: Data from patients who were excluded from the study

Patients excluded from the study		**n**
Patients treated in other hospitals		22
Patients without an MRI examination		33
MRI without DWI		5
Patients who received invasive treatment before MRI		18
Poor image quality		9
Pathologically confirmed other than IPAC or PPAC	neuroendocrine tumor	12
	gastrointestinal stromal tumor	7
	squamous cell carcinoma with ampullary adenocarcinoma	3
	high-grade pancreatic intraepithelial neoplasia	4

MRI: magnetic resonance imaging; DWI: Diffusion-weighted imaging; IPAC: intestinal-type periampullary adenocarcinoma; PPAC: pancreatobiliary-type periampullary adenocarcinoma

MRI was conducted using a 1.5-T MR system (Verio; Siemens Medical Solutions, Erlangen, Germany). With b-values of 1000 s/mm^2, diffusion-weighted imaging was performed. The imaging protocol consisted of acquiring thin-section turbo spin-echo T2-weighted (TSE) images in the sagittal, coronal, and transverse planes. A total of 20 slices were obtained, each with a thickness of 4 mm and no intersection gap. The imaging parameters for the TSE sequence were specific: (1) repetition time (TR) of 6000 ms, (2) echo time (TE) of 150 ms, and (3) the number of signals acquired of 2. The resulting picture resolution was 0.8 mm x 0.8 mm. For diffusion-weighted imaging, axial plane acquisitions were conducted using respiratory-triggered single-shot echo-planar sequences. The acquisition parameters were a matrix size of 180 x 200, a field of view (FOV) ranging

from 40 to 44 cm, a slice thickness of 4 mm, an intersection gap of 1 mm, a bandwidth of 350 kHz/pixel, an acquisition duration of 6-8 minutes, a flip angle of 90°, and the number of excitations (NEX) of 5.

Image Analysis

The DWI raw data were transferred from the picture archiving and communication system (PACS) to a personal computer (PC) for processing using the open-source LIFEx 7.3.0 voxel program (https://lifesoft.org). Two radiologists with 14 and eight years of experience, respectively, who were blind to the pathological results independently reviewed all MRI images. The researchers manually outlined the ROI using T2-weighted axial images as a guide. The voxel data were automatically aggregated to create a volumetric ROI encompassing the whole tumor. A volumetric ADC map was then created (Figure 1).

Figure 1: An example of manually drawn regions of interest (ROIs) on the apparent diffusion coefficient (ADC) maps for evaluating the volumetric ADC histogram analysis of the periampullary adenocarcinomas. The whole tumor was manually evaluated as an ROI for each slice of the ADC map. The axial T2-weighted and contrast-enhanced images were referred to for details.

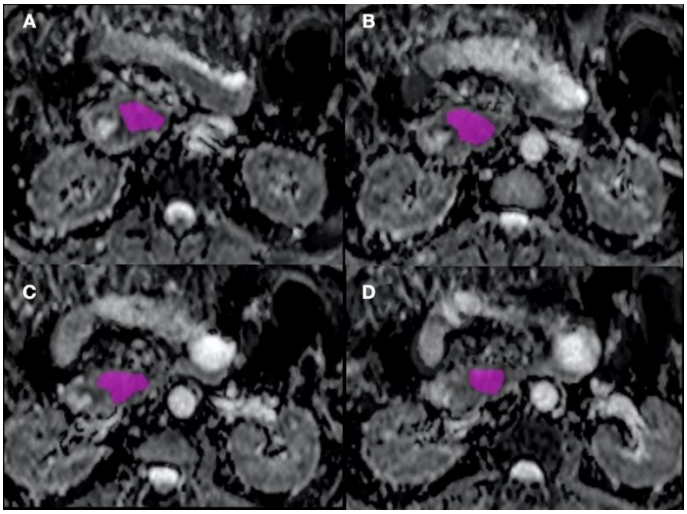

The study involved determination of various statistical measures for ADC values, including the 5^{th}, 10^{th}, 25^{th}, 50^{th}, 75^{th}, 90^{th}, and 95^{th} percentiles. Additionally, the study examined the ADC_{max}, ADC_{mean}, ADC_{median}, and ADC_{min} values in addition to variance, kurtosis, and skewness. The n^{th} percentile represents the threshold at which n% of the voxel values from the histogram were seen on the lower end. Skewness indicates that the distribution possesses a rightward tail that is either flatter or longer in comparison to the leftward tail. Kurtosis is a statistical measure that quantifies the degree of peakedness in the distribution of a histogram. A high kurtosis value indicates a prominent peak near the mean, a rapid decline in values away from the peak, and heavy tails in the distribution.

Statistical analysis

Statistical analysis was performed using IBM SPSS 23.0 software (Chicago, IL, USA). Histograms were constructed from the combined ADC values of patients in the well-differentiated and poorly differentiated groups of IPAC and PPAC. The histograms demonstrated that the distribution of all measurements varied. Based on the measurements, descriptive statistics were performed for every set of patients, including measures such as mean, minimum, median, maximum, standard deviation, skewness, kurtosis, and percentiles. These descriptive data were then visually represented to illustrate the variances among the patient groups. The statistics from the previously mentioned group were computed based on data pertaining to individual participants. The t-test for independent samples was employed to assess the potential differences in the statistics obtained from individuals across various groups. Receiver operating characteristic (ROC) curves were produced based on individual statistics, and the cut-off parameters for the resulting statistics were computed.

Results

Population Information

Fifteen cumulative instances were incorporated in the IPAC group, consisting of 11 well-differentiated cases (as shown in Figure 2) and four poorly differentiated cases (as shown in Figure 3). Similarly, the PPAC group comprised 54 cases with 45 well-differentiated cases (as depicted in Figure 4) and nine poorly differentiated cases (as illustrated in Figure 5). The study consisted of a total of 44 male participants and 25 female participants. No statistically significant differences in terms of gender (P=0.555) or age (P=0.560) were found (Table 2).

Figure 2: A 67-year-old female patient with well-differentiated intestinal-type periampullary adenocarcinoma (IPAC). The lesion was isointense (white arrow) on the axial T2-weighted images (a), and the double duct sign was observed on the magnetic resonance cholangiopancreatography (MRCP) (b) image. The lesion showed progressive enhancement (white arrows) in the contrast-enhanced magnetic resonance imaging (MRI) sequences (c,d). The diffusion-weighted image (DWI) as shown in indicated hyperintensity, and the apparent diffusion coefficient image (f) showed hypointensity consistent with diffusion restriction (white arrows).

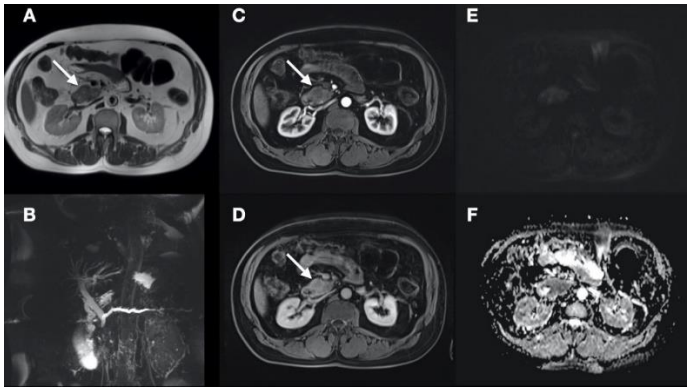

Figure 3: A 54-year-old male patient with poorly differentiated IPAC. The lesion displayed hyperintensity (white arrows) on the T2-weighted images (a–b) and continuous enhancement (white arrows) in the contrast-enhanced MRI sequences (c–d). Diffusion restriction was observed on the DWIs (e,f).

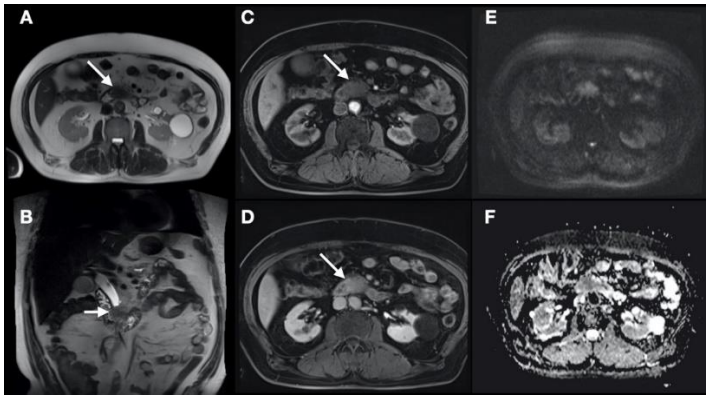

Figure 4: A 73-year-old male patient with well-differentiated pancreatobiliary-type periampullary adenocarcinoma (PPAC). The lesion was hyperintense (white arrow) on T2-weighted images (a), hypointense (white arrow) on T1-weighted images (b) and showed progressive enhancement (white arrows) on the (c,d) contrast-enhanced MRI sequences. The DWI (e) demonstrated hyperintensity, while the apparent diffusion coefficient image (f) exhibited hypointensity, both of which indicate diffusion restriction.

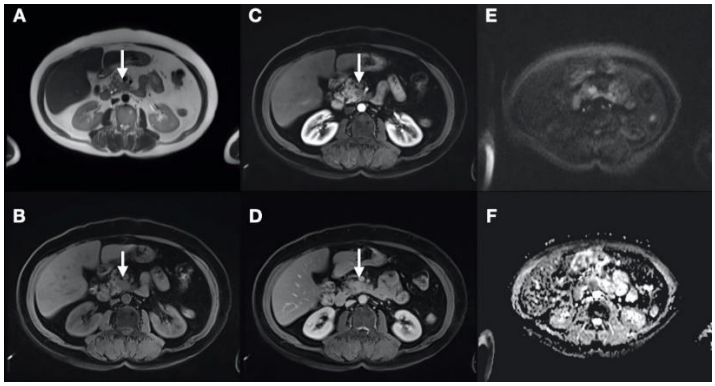

Figure 5: A 58-year-old female patient with poorly differentiated intestinal-type periampullary adenocarcinoma. The lesion was hyperintense (white arrow) on the axial T2-weighted images (a), and MRCP (b) images showed that the common bile duct has an abrupt ending. On contrast-enhanced MRI sequences, the lesion exhibited gradual enhancement (white arrows as shown in c,d). On the DWIs, diffusion restriction was detected (e,f).

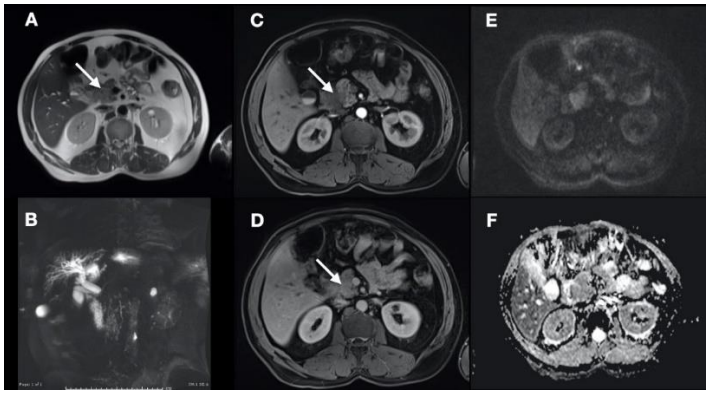

Interobserver agreement

The assessment of agreement between the two observers was conducted utilizing the interclass correlation coefficient (ICC). All metrics exhibited ICCs that surpassed the threshold of 0.8, signifying a high level of agreement that approached perfection.

Tumor diameter results

While no difference in tumor size between well- and poorly differentiated groups for intestinal-type periampullary carcinomas was detected, the poorly differentiated group had a greater tumor diameter than the well-differentiated group (P=0.044) for pancreatic-type periampullary adenocarcinomas (Table 1).

ADC histogram parameters results

The ADC_{min}, ADC_{mean}, ADC_{median}, and ADC_{max} together with the percentiles of ADC values in the poorly differentiated group exhibited lower values when compared with those of the well-differentiated group in both PPAC and IPAC patients. However, the difference between the two groups was not statistically significant. No significant distinction could be observed between the variance and skewness metrics. Kurtosis in patients with IPAC was found to be significantly higher in the well-differentiated group (P=0.048) when compared with the poorly differentiated group. The descriptive features of both well-differentiated and poorly differentiated groups of both types of periampullary carcinoma patients are summarized in Tables 2 and 3.

The ROC curve demonstrated the effectiveness of the histogram settings for determining differentiation degree of periampullary carcinomas. In IPAC patients, the greatest value for the area under the curve (AUC) of kurtosis was found to be 0.818. When the cut-off value was set at 0.123, the sensitivity and specificity were observed to be 75% and 90%, respectively.

Table 2: Demographic, radiological, and pathological data of IPAC and PPAC patients

			Well-differentiated	Poorly differentiated	
			n (%) / mean (SD)	n (%) / mean (SD)	*P*-value
IPAC	Age		66.18 (9.14)	65 (4.24)	0.555[a]
	Sex	Male	8 (72.7)	2 (50.0)	0.560[b]
		Female	3 (27.3)	2 (50.0)	
	Tumor diameter (mm)		20.22 (6.94)	19.37 (11.82)	0.695[a]
PPAC	Age		60.78 (8.24)	63.33 (7.48)	0.416a
	Sex	Male	27 (60.0)	7 (77.8)	0.458[b]
		Female	3 (27.3)	2 (22.2)	
	Tumor diameter (mm)		24.99 (8.62)	32.33 (11.83)	0.044[a]

[a] Mann–Whitney U Test; [b]Chi-squared test. IPAC: intestinal-type periampullary adenocarcinoma; PPAC: pancreatobiliary-type periampullary adenocarcinoma, SD: standard deviation

Table 3: Comparisons of apparent diffusion coefficient (ADC) histogram parameters between well-differentiated and poorly differentiated IPAC groups.

ADC (10^{-3} mm^2/s)	Well-differentiated	Poorly differentiated	Total	*P*-value
Mean	1.277 (0.372)	1.177 (0.198)	1.204 (0.244)	0.514
SD	0.212 (0.56)	0.233 (0.74)	0.228 (0.686)	0.602
Median	1.279 (0.365)	1.153 (0.200)	1.186 (0.246)	0.514
Minimum	0.783 (0.358)	0.723 (0.257)	0.739 (0.274)	0.794
Maximum	1.760 (0.384)	1.783 (0.288)	1.777 (0.301)	0.896
Skewness	−0.5 (0.3)	−0.5 (0.5)	−0.5 (0.5)	0.896
Kurtosis	0.0 (0.3)	0.3 (0.3)	0.2 (0.3)	0.048
5th	0.920 (0.283)	0.834 (0.232)	0.858 (0.239)	0.896
10th	0.997 (0.309)	0.891 (0.232)	0.919 (0.248)	0.695
25th	1.119 (0.339)	0.988 (0.223)	1.023 (0.252)	0.514
50th	1.279 (0.365)	1.153 (0.200)	1.186 (0.246)	0.514
75th	1.450 (0.420)	1.358 (0.218)	1.383 (0.271)	0.695
90th	1.577 (0.457)	1.501 (0.232)	1.521 (0.291)	0.695
95th	1.623 (0.464)	1.585 (0.217)	1.595 (0.283)	0.896

ADC: apparent diffusion coefficient, SD: standard deviation

Table 4: Comparisons of ADC histogram parameters between well-differentiated and poorly differentiated groups of PPAC patients

ADC (10^{-3} mm^2/s)	Well-differentiated	Poorly differentiated	Total	*P*-value
Mean	1.314 (0.241)	1.287 (0.306)	1.310 (0.250)	0.359
SD	0.194 (0.46)	0.200 (0.37)	0.195 (0.45)	0.702
Median	1.306 (0.249)	1.275 (0.318)	1.300 (0.258)	0.275
Minimum	0.822 (0.242)	0.748 (0.267)	0.810 (0.245)	0.236
Maximum	1.878 (0.314)	1.832 (0.362)	1.870 (0.319)	0.523
Skewness	0.2 (0.4)	0.1 (0.4)	0.1 (0.4)	0.944
Kurtosis	0.1 (0.6)	−0.2 (0.5)	0.0 (0.6)	0.280
5th	1.010 (0.219)	0.967 (0.245)	1.003 (0.222)	0.223
10th	1.069 (0.222)	1.036 (0.262)	1.063 (0.227)	0.313
25th	1.178 (0.238)	1.147 (0.321)	1.173 (0.250)	0.246
50th	1.306 (0.249)	1.275 (0.318)	1.300 (0.258)	0.275
75th	1.441 (0.258)	1.426 (0.317)	1.438 (0.265)	0.472
90th	1.570 (0.263)	1.552 (0.334)	1.567 (0.273)	0.451
95th	1.650 (0.270)	1.633 (0.338)	1.647 (0.279)	0.451

ADC: apparent diffusion coefficient, SD: standard deviation

Discussion

This study provides a novel investigation into the potential implications of volumetric ADC histogram analysis as no prior research has been conducted for determining the degree of differentiation of periampullary tumors. Histogram parameters that are generated from ADC maps can provide data about the intrinsically pathogenic aspects of pancreatic adenocarcinomas have been extensively studied, revealing significant advancements in terms of enhanced characterization and prognosis according to previous research.

To verify the diagnosis, imaging techniques can effectively detect and localize focal periampullary tumors. Furthermore, imaging techniques are of paramount importance in the determination of therapy allocation for patients as they provide valuable insights into the local tumor stage and the exclusion of distant metastases [15,16]. Multi-detector computed

tomography (MDCT) is the most often used imaging modality followed by MRI and magnetic resonance cholangiopancreatography (MRCP).

The 5-year survival rate of resectable periampullary carcinomas is reported to be 20%–50%. Hence, adjuvant treatment has been suggested to increase overall survival; however, adjuvant treatment may be costly and ineffective. No realistic adjuvant treatment guidelines exist since a lack of consensus regarding the optimal and efficacious chemotherapy protocol and limited data is not available [17].

The intestinal transcription factor, known as CDX2, plays a crucial role in histological identification of challenging instances. Histological subtypes can be differentiated by the presence of mucin (MUC2) and intermediate filament biomarkers [18]. This marker's expression predicts longer overall survival independent of morphology [19]. In addition, some chromosomal abnormalities, such as the gains of 13q and 3q and the deletion of 5q, were detected to be specific to IPAC [20–22]. Nevertheless, it is impossible to examine these characteristics of periampullary carcinomas prior to surgery.

The characteristics of ADC are associated with various aspects of the tumor microenvironment, such as cell membrane stability, cellular proliferation rate, and extracellular matrix composition. The resulting phenomenon exhibits a resemblance to the Brownian motion of water particles [23,24]. Within the range of b-values ranging from 200 to 1000 s/mm^2, the signal attenuation associated with diffusion exhibits a linear pattern, which aligns with the principles of Gaussian diffusion. Non-Gaussian diffusion is observed when b-values exceed 1000 s/mm^2, leading to a commensurate decrease in the ADC value [25]. The primary objective of our investigation was the examination of volumetric ADC histograms and its utility in discerning the differentiation level between well-differentiated and poorly differentiated groups among patients with IPAC and PPAC. It was observed that the ADC values of the poorly differentiated groups, specifically the percentiles of ADC values in addition to ADC_{min}, ADC_{median}, ADC_{mean}, and ADC_{max}, exhibited lower values compared to the highly differentiated groups. However, the difference between the groups was not statistically significant. Kurtosis of ADC was a significant predictor of IPAC differentiation degree. The carcinoma was more likely to be poorly differentiated if the skewness was greater than 0.2.

According to the findings of Shindo et al. [26], utilization of ADC histogram-derived characteristics proved to be effective in differentiating between pancreatic neuroendocrine neoplasms and pancreatic ductal adenocarcinomas. Pancreatic neuroendocrine neoplasms had considerably higher mean ADC_{200} and ADC_{400} values. Pancreatic ductal adenocarcinomas demonstrated elevated levels of skewness and kurtosis when assessed with ADC_{400}. The study conducted by Lu et al. [14] determined that the maximum area under the curve (AUC) for differentiating between IPAC and PPAC was observed at the 75th percentile with an AUC value of 0.781. The sensitivity and specificity were found to be 91% and 59%, respectively, with a cut-off value of 1.50 x 10^{-3} mm²/s. In their study, Bi et al. [27] revealed that the average ADC was not able to differentiate these groups. However, they noticed that the ADC_{min} showed potential in terms of differentiating between the groups with a sensitivity of 85.2%, specificity of 50%, and an AUC of 0.672.

One of the most salient features of the study of the ADC histogram is the assessment of the biological activity of pancreatic cancer. Previous studies have indicated that a range of ADC histogram metrics have the potential to detect cancers exhibiting unfavorable clinical characteristics and a poor prognosis [28–31]. The study conducted by De Robertis et al. [30] demonstrated that the entropy of the ADC was significantly elevated in G2-3 pancreatic neuroendocrine neoplasms. The AUC for these neoplasms was found to be 0.757, indicating moderate discriminatory power. The sensitivity and specificity of the ADC entropy in differentiation between G2 and G3 pancreatic neuroendocrine neoplasms were determined to be 83.3% and 61.1%, respectively. Pereira et al. [28] reported a correlation between the histological grade of pancreatic neuroendocrine tumors and data from the histogram analysis. The average ADC and the 75th, 90th, and 95th percentiles exhibited notably higher values in G1 tumors when compared with either G2 or G3 cancers. Additionally, substantial differences in the skewness and kurtosis measures were found between G1 and G3 tumors.

The whole-lesion ADC entropy, the mean of the bottom 10th percentile, and the mean of the 10th–25th percentile indicated substantial variations between benign and malignant pancreatic intraductal papillary mucosal neoplasms (IPMNs) as reported by Hoffman et al. [29]. ADC entropy was the most effective parameter for predicting malignancy with 83% accuracy, 100% sensitivity, and 70% specificity. A study conducted by Igarashi et al. [32] provided evidence supporting the accurate prediction of high-grade dysplasia in IPMNs with the use of ADC entropy, achieving an accuracy rate of 73%.

In previous research, an ADC histogram analysis was used to compare neoplastic processes to periampullary adenocarcinomas. While misdiagnosis might lead to unnecessary and invasive surgery, the imaging properties of mass-forming pancreatitis based on the use of MRI are essential for differentiating pancreatitis from adenocarcinomas [33–36]. Many researchers have reported different ADC optimum threshold values, ranging from 0.88 to 1.26 10^{-3} mm^2/s to distinguish mass-forming autoimmune pancreatitis (AIP) from PDAC [37–41].

Limitations

This study has some strengths and limitations. This work describes the initial investigation into the possible usefulness of volumetric ADC histogram analysis based on the available knowledge in determining the degree of differentiation of periampullary carcinomas. In this study, the patients were chosen using a retrospective analytic methodology, which presents the potential for bias. We evaluated only the ADC parameters generated from higher b-values as no significant differences between investigations with lower b values could be found. Patients who were too advanced to receive surgery were excluded from the study. Additional research is required to substantiate the results of this research.

Conclusion

This research suggests that the kurtosis of ADC is a reliable indicator of IPAC's differentiation degree. When the kurtosis was >0.2, the carcinoma was more likely to be poorly

differentiated. The utilization of the analysis of volumetric ADC histograms may offer a noninvasive method for assessing the degree of differentiation in IPACs prior to surgical intervention and provide information about patients' prognosis and treatment management.

References

1. Sarmiento JM, Nagomey DM, Sarr MG, Farnell MB. Periampullary cancers: are there differences? Surg Clin North Am. 2001;81:543-55.
2. Fernandez-Cruz L. Periampullary carcinoma. In: Holzheimer RG, Mannick JA, editors. Surgical Treatment: Evidence-Based and Problem-Oriented. Munich: Zuckschwerdt; 2001.
3. Surveillance, Epidemiology, and End Results Program, Cancer Stat Facts: Pancreatic Cancer. NIH. 2022.
4. Conroy T, Hammel P, Hebbar M, Ben Abdelghani M, Wei AC, Raoul JL, et al. Canadian Cancer Trials Group and the Unicancer-GI–PRODIGE Group. FOLFIRINOX or Gemcitabine as Adjuvant Therapy for Pancreatic Cancer. N Engl J Med. 2018;379:2395-406.
5. Ducreux M, Cuhna AS, Caramella C, Hollebecque A, Burtin P, Goéré D, et al. ESMO Guidelines Committee. Cancer of the pancreas: ESMO Clinical Practice Guidelines for diagnosis, treatment and follow-up. Ann Oncol. 2015;26:56-68.
6. Williams JL, Chan CK, Toste PA, Elliott IA, Vasquez CR, Sunjaya DB, et al. Association of Histopathologic Phenotype of Periampullary Adenocarcinomas With Survival. JAMA Surg. 2017;152:82-8.
7. Westgaard A, Tafjord S, Farstad IN, Cvancarova M, Eide TJ, Mathisen O, et al. Pancreatobiliary versus intestinal histologic type of differentiation is an independent prognostic factor in resected periampullary adenocarcinoma. BMC Cancer. 2008;8:170.
8. Bronsert P, Kohler I, Werner M, Makowiec F, Kuesters S, Hoeppner J, et al. Intestinal-type of differentiation predicts favourable overall survival: confirmatory clinicopathological analysis of 198 periampullary adenocarcinomas of pancreatic, biliary, ampullary and duodenal origin. BMC Cancer. 2013;13:428.
9. Nishio K, Kimura K, Amano R, Yamazoe S, Ohrira G, Nakata B et al. Preoperative predictors for early recurrence of resectable pancreatic cancer. World J Surg Oncol. 2017;15:16.
10. Endo Y, Fujimoto M, Ito N, Takahashi Y, Kitago M, Gotoh M, et al. Clinicopathological impacts of DNA methylation alterations on pancreatic ductal adenocarcinoma: prediction of early recurrence based on genome-wide DNA methylation profiling. J Cancer Res Clin Oncol. 2021;147:1341-1354.
11. Hasan S, Jacob R, Manne U, Paluri R. Advances in pancreatic cancer biomarkers. Oncol Rev. 2019;13:410.
12. Just N. Improving tumour heterogeneity MRI assessment with histograms. Br J Cancer. 2014;111:2205-13.
13. Li A, Xing W, Li H, Hu Y, Hu D, Li Z, et al. Subtype Differentiation of Small (≤ 4 cm) Solid Renal Mass Using Volumetric Histogram Analysis of DWI at 3-T MRI. AJR Am J Roentgenol. 2018;211:614-23.
14. Lu JY, Yu H, Zou XL, Li Z, Hu XM, Shen YQ, et al. Apparent diffusion coefficient-based histogram analysis differentiates histological subtypes of periampullary adenocarcinoma. World J Gastroenterol. 201928;25:6116-28.
15. Kamarajah SK. Pancreaticoduodenectomy for periampullary tumours: a review article based on Surveillance, End Results and Epidemiology (SEER) database. Clin Transl Oncol. 2018;20:1153-1160.
16. Al-Hawary MM, Kaza RK, Francis IR. Optimal Imaging Modalities for the Diagnosis and Staging of Periampullary Masses. Surg Oncol Clin N Am. 2016;25:239-53.
17. Acharya A, Markar SR, Sodergren MH, Malietzis G, Darzi A, Athanasiou T, et al. Meta-analysis of adjuvant therapy following curative surgery for periampullary adenocarcinoma. Br J Surg. 2017;104:814-22.
18. Kumari N, Prabha K, Singh RK, Baitha DK, Krishnani N. Intestinal and pancreatobiliary differentiation in periampullary carcinoma: the role of immunohistochemistry. Hum Pathol. 2013;44:2213-9.
19. Zhou H, Schaefer N, Wolff M, Fischer HP. Carcinoma of the ampulla of Vater: comparative histologic/immunohistochemical classification and follow-up. Am J Surg Pathol. 2004;28:875-82.
20. Sandhu V, Bowitz Lothe IM, Labori KJ, Lingjærde OC, Buanes T, Dalsgaard AM, et al. Molecular signatures of mRNAs and miRNAs as prognostic biomarkers in pancreatobiliary and intestinal types of periampullary adenocarcinomas. Mol Oncol. 2015;9:758-71.
21. Sandhu V, Wedge DC, Bowitz Lothe IM, Labori KJ, Dentro SC, Buanes T, et al. The Genomic Landscape of Pancreatic and Periampullary Adenocarcinoma. Cancer Res. 2016;76:5092-102.
22. Kalluri Sai Shiva UM, Kuruva MM, Mitnala S, Rupjyoti T, Guduru Venkat R, Botlagunta S, et al. MicroRNA profiling in periampullary carcinoma. Pancreatology. 2014;14:36-47.
23. Surov A, Meyer HJ, Wienke A. Correlation between apparent diffusion coefficient (ADC) and cellularity is different in several tumors: a meta-analysis. Oncotarget. 2017;8:59492-9.
24. Meyer HJ, Leifels L, Hamerla G, Höhn AK, Surov A. ADC-histogram analysis in head and neck squamous cell carcinoma. Associations with different histopathological features including expression of EGFR, VEGF, HIF-1α, Her 2 and p53. A preliminary study. Magn Reson Imaging. 2018;54:214-7.
25. Iima M, Le Bihan D. Clinical Intravoxel Incoherent Motion and Diffusion MR Imaging: Past, Present, and Future. Radiology. 2016;278:13-32.
26. Shindo T, Fukukura Y, Umanodan T, Takumi K, Hakamada H, Nakajo M, et al. Histogram Analysis of Apparent Diffusion Coefficient in Differentiating Pancreatic Adenocarcinoma and Neuroendocrine Tumor. Medicine (Baltimore). 2016;95:2574.
27. Bi L, Dong Y, Jing C, Wu Q, Xiu J, Cai S, et al. Differentiation of pancreatobiliary-type from intestinal-type periampullary carcinomas using 3.0T MRI. J Magn Reson Imaging. 2016;43:877-86.
28. Pereira JA, Rosado E, Bali M, Metens T, Chao SL. Pancreatic neuroendocrine tumors: correlation between histogram analysis of apparent diffusion coefficient maps and tumor grade. Abdom Imaging. 2015;40:3122-8.
29. Hoffman DH, Ream JM, Hajdu CH, Rosenkrantz AB. Utility of whole-lesion ADC histogram metrics for assessing the malignant potential of pancreatic intraductal papillary mucinous neoplasms (IPMNs). Abdom Radiol (NY). 2017;42:1222-8.
30. De Robertis R, Maris B, Cardobi N, Tinazzi Martini P, Gobbo S, Capelli P, et al. Can histogram analysis of MR images predict aggressiveness in pancreatic neuroendocrine tumors? Eur Radiol. 2018;28:2582-91.
31. De Robertis R, Beleù A, Cardobi N, Frigerio I, Ortolani S, Gobbo S, et al. Correlation of MR features and histogram-derived parameters with aggressiveness and outcomes after resection in pancreatic ductal adenocarcinoma. Abdom Radiol (NY). 2020;45:3809-18.
32. Igarashi T, Shiraishi M, Watanabe K, Ohki K, Takenaga S, Ashida H, et al. 3D quantitative analysis of diffusion-weighted imaging for predicting the malignant potential of intraductal papillary mucinous neoplasms of the pancreas. Pol J Radiol. 2021;86:298-308.
33. Agrawal S, Daruwala C, Khurana J. Distinguishing autoimmune pancreatitis from pancreaticobiliary cancers: current strategy. Ann Surg. 2012;255:248-58.
34. Kim JH, Kim MH, Byun JH, Lee SS, Lee SJ, Park SH, et al. Diagnostic Strategy for Differentiating Autoimmune Pancreatitis From Pancreatic Cancer: Is an Endoscopic Retrograde Pancreatography Essential? Pancreas. 2012;41:639-47.
35. Hedfi M, Charfi M, Nejib FZ, Benlahouel S, Debaibi M, Ben Azzouz S, et al. Focal Mass-Forming Autoimmune Pancreatitis Mimicking Pancreatic Cancer: Which strategy? Tunis Med. 2019;97:731-5.
36. Wolske KM, Ponnatapura J, Kolokythas O, Burke LMB, Tappouni R, Lalwani N. Chronic Pancreatitis or Pancreatic Tumor? A Problem-solving Approach. Radiographics. 2019;39:1965-82.
37. Hur BY, Lee JM, Lee JE, Park JY, Kim SJ, Joo I, et al. Magnetic resonance imaging findings of the mass-forming type of autoimmune pancreatitis: comparison with pancreatic adenocarcinoma. J Magn Reson Imaging. 2012;36:188-97.
38. Choi SY, Kim SH, Kang TW, Song KD, Park HJ, Choi YH. Differentiating Mass-Forming Autoimmune Pancreatitis From Pancreatic Ductal Adenocarcinoma on the Basis of Contrast-Enhanced MRI and DWI Findings. AJR Am J Roentgenol. 2016;206:291-300.
39. Muhi A, Ichikawa T, Motosugi U, Sou H, Sano K, Tsukamoto T, et al. Mass-forming autoimmune pancreatitis and pancreatic carcinoma: differential diagnosis on the basis of computed tomography and magnetic resonance cholangiopancreatography, and diffusion-weighted imaging findings. J Magn Reson Imaging. 2012;35:827-36.
40. Kamisawa T, Takuma K, Anjiki H, Egawa N, Hata T, Kurata M, et al. Differentiation of autoimmune pancreatitis from pancreatic cancer by diffusion-weighted MRI. Am J Gastroenterol. 2010;105:1870-5.
41. Jia H, Li J, Huang W, Lin G. Multimodel magnetic resonance imaging of mass-forming autoimmune pancreatitis: differential diagnosis with pancreatic ductal adenocarcinoma. BMC Med Imaging. 2021;21:149.